JOURNAL OF BACTERIOLOGY, Dec. 1983, p. 1282–1291
0021-9193/83/121282-10$02.00/0

Vol. 156, No. 3

Structural Heterogeneity in Populations of the Budding Yeast *Saccharomyces cerevisiae*

MARCO VANONI, MARINA VAI, LAURA POPOLO, AND LILIA ALBERGHINA*

Sezione di Biochimica Comparata, Dipartimento di Fisiologia e Biochimica Generali, Università di Milano, 20133 Milan, Italy

Received 8 June 1983/Accepted 23 August 1983

Bud scar analysis integrated with mathematical analysis of DNA and protein distributions obtained by flow microfluorometry have been used to analyze the cell cycle of the budding yeast *Saccharomyces cerevisiae*. In populations of this yeast growing exponentially in batch at 30°C on different carbon and nitrogen sources with duplication times between 75 and 314 min, the budded period is always shorter (approximately 5 to 10 min) than the sum of the S + G2 + M + G1* phases (determined by the Fried analysis of DNA distributions), and parent cells always show a prereplicative unbudded period. The analysis of protein distributions obtained by flow microfluorometry indicates that the protein level per cell required for bud emergence increases at each new generation of parent cells, as observed previously for cell volume. A wide heterogeneity of cell populations derives from this pattern of budding, since older (and less frequent) parent cells have shorter generation times and produce larger (and with shorter cycle times) daughter cells. A possible molecular mechanism for the observed increase with genealogical age of the critical protein level required for bud emergence is discussed.

The asymmetrical cell division of *Saccharomyces cerevisiae* has been extensively investigated by time-lapse cinephotomicrography experiments and by bud scar analysis (6, 13, 18, 19, 20, 29, 30). The results of these experiments may be interpreted by assuming that cells need to attain a critical size to initiate the cycle, a regulatory step that requires the execution of the CDC28 event and commits the cell to DNA replication and cell division (12, 18, 24, 29). Such a critical cell size model implies defined relationships between growth metabolism—more specifically, protein accumulation (23)—and the nuclear division cycle (1, 3).

These relations may be more carefully evaluated by using the recently developed flow microfluorometry technique, which allows the experimental determination of the frequency functions of DNA, protein, and RNA contents of individual cells on significant samples (10^5 to 10^6 cells) of microbial populations (4, 11). In fact, these functions are determined by the law of growth of the individual cells, the structure of the population, and the variability of the momentary size distribution (33). It has been found that cell sizes at a given age (for instance, at budding or at division) are distributed around a mean value according to a function (the momentary size distribution) that can be well represented by a Gaussian function with a coefficient of variation (CV) generally in the range of 20% (15, 32). Computer programs that take into account the experimental variability may thus make it possible to extract the law of growth of the single cell or the structure of the population from the experimental frequency functions in a statistically significant manner.

Relevant information on cell cycle dynamics may thus be obtained on sizable samples of unperturbed populations in balanced exponential growth in shaken liquid cultures, thereby overcoming the uncertainties given by the analysis of the synchronized populations (21, 22) and by the investigation of a small number of cells growing in an unusual environment, as in the time-lapse cinematography experiments.

MATERIALS AND METHODS

The haploid strain S288c (*MATα SUC2 mal gal2 CUP1*) of *S. cerevisiae*, kindly provided by Dr. S. Sora (Istituto di Genetica, Università di Milano), was used throughout this study. Cells were grown in two types of basal medium: the first (YEP) contained (per liter of medium) 10 g of yeast extract, 20 g of Bacto-Peptone, and 20 g of carbon source (YEP-gluconate medium was buffered to pH 5.8 with orthophosphoric acid), and the second type (YNB) contained (per liter of medium) 6.7 g of yeast nitrogen base (Difco) without amino acids and 40 g of the carbon source. When glutamine (500 mg/liter) was used as the sole nitrogen source, Difco YNB without amino acids and ammoni-

um sulfate was used. Flasks (750 ml) containing 200 ml of medium were inoculated with fresh yeast cells and incubated in a Dubnoff water bath with shaking at 30°C. Growth was monitored as the increase in cell number, and the rate constant of exponential growth, α (min^{-1}) = ln2/T, where T is the duplication time of the culture, was determined by linear regression on a semilogarithmic plot.

Determination of cell number and cell volume distributions. The number of cells present in small samples of cell culture diluted with Isoton (Coulter Electronics, Harpenden, United Kingdom) and mildly sonicated was determined by the use of a Coulter model ZBI Counter with a 100-μm orifice tube. Mean cell volume ($\bar{V}$) was estimated from the cell volume distributions obtained with a Coulter Channalyzer C-1000 by use of the equation

$$\bar{V} = (\Sigma n_i \cdot c_i/\Sigma n_i) \cdot F \quad (1)$$

where n_i is the number of cells contained in the c_i channel ($0 < i < 100$) and F is a calibration factor. The equipment was calibrated by the use of 8.9-μm-diameter latex spheres (Coulter Electronics).

Determination of the percentage of budded and of binucleate cells. The percentage of total budded cells was determined by direct microscopic counting on at least 400 cells that had been fixed in 10% Formalin and mildly sonicated. After staining with 0.2% Calcofluor (a gift from E. Cabib, National Institutes of Health, Bethesda, Md.), at least 1,000 cells were scored under a Leitz Dialux Fluorescence microscope at ×1,000 and assigned to one of the following classes: (i) unbudded daughters; (ii) budded daughters; (iii) unbudded parents; (iv) budded parents.

The percentage of binucleated G1* cells, with two nuclei with presynthetic DNA content (cells between mitosis and cell division), was determined after at least 20 min of staining with 1 μg of 4′,6′-diamino-2-phenylindole · 2HCl (DAPI) per ml in phosphate-buffered saline (PBS). At least 400 cells were scored for each determination under a Leitz Dialux fluorescence microscope at ×1,000.

Determination of the duration of cell cycle phases, budded period, and parent and daughter generation times. The formulas used to calculate T_B, the length of the budded period, which is of appreciable constant duration in both parent and daughter cells (18, 19), T_P (the average parent cycle time), and T_D (the average daughter cycle time) are as follows.

$$T_B = \log_2 (1 + F_B) \cdot T \quad (2)$$

$$T_P = \log_2 (F_B/F_{PB}) \cdot T \quad (3)$$

$$T_D = \log_2 (F_B/F_{DB}) \cdot T \quad (4)$$

where F_B is the percentage of budded cells, and F_{PB} and F_{DB} are the fractions of budded parents and daughters, respectively, on the whole population, determined by bud scar analysis.

Let $F_{S+G2+M+G1^*} = F_\Sigma$ and $F_{G2+M+G1^*}$ be the fractions of cells between initiation or completion of DNA synthesis, respectively, and cell division, as judged by Fried's deconvolution of DNA histograms obtained by flow cytometry. An estimation of T_Σ and $T_{G2+M+G1^*}$ is given by

$$T_\Sigma = \log_2 (1 + F_\Sigma) \cdot T \quad (5)$$

$$T_{G2+M+G1^*} = \log_2 (1 + F_{G2+M+G1^*}) \cdot T \quad (6)$$

By similar reasoning, T_{G1^*} is given by

$$T_{G1^*} = \log_2 (1 + F_{G1^*}) \cdot T \quad (7)$$

where F_{G1^*} is the fraction of binucleate cells. By subtracting equation 7 from equation 6, T_{G2+M} is given by

$$T_{G2+M} = \log_2 \left(\frac{1 + F_{G2+M+G1^*}}{1 + F_{G1^*}} \right) \cdot T \quad (8)$$

Similarly, subtraction of equation 6 from equation 5 gives the average duration of the DNA synthetic phase:

$$T_S = \log_2 \left(\frac{1 + F_\Sigma}{1 + F_{G2+M+G1^*}} \right) \cdot T \quad (9)$$

Because of the unequal mode of division of *S. cerevisiae*, no meaningful length of G1 phase on the whole population may be calculated from flow cytometric data.

Flow cytometric analysis. Samples of cells were mildly sonicated, collected by centrifugation, washed, and suspended in 70% ethanol before analysis. To obtain protein distributions, *S. cerevisiae* cells were washed once with PBS (pH 7.4) and then were stained with 50 μg of fluorescein isothiocyanate per ml in 0.5 M sodium bicarbonate. After 30 min in ice, cells were recovered and washed three times with PBS (2, 7). The intensity of green fluorescence (>520 nm) was measured on at least 10^5 cells with a FACS IV fluorescence-activated cell sorter (Becton, Dickinson & Co.) equipped with a 5-W argon ion laser which yielded ca. 400 mW at 488 nm in our conditions. For DNA staining, cells were washed once with PBS, treated with RNase (1 mg/ml) for 90 min at 37°C, washed with PBS, and suspended in 50 mM Tris (pH 7.7) containing 15 mM $MgCl_2$ and 46 mM propidium iodide (23). After at least 20 min of staining in ice, cells were directly examined, and total fluorescence intensity was measured as described above on at least 10^5 cells. By this procedure, fluorescence is collected by a light detector which transmits an electric pulse whose height is proportional to the fluorescence intensity; under our staining conditions it is also proportional to the protein or DNA content per cell. Each pulse is stored in a multichannel analyzer. In this way, the frequency distribution functions of protein and of DNA content are obtained at the end of the run.

Protein and DNA distribution analysis. Protein distribution was analyzed by a computer program developed in our laboratory. First, from the age density function of the population and from the assumptions made on the behavior of the threshold required for budding at the different genealogical ages, the ideal protein density function (i.e., the frequency of cells in a population with a given protein content), which is stable in balanced exponential growth, was calculated as described in the appendix. Then, given the ideal protein density function, the program took into account variability in size for cells at any given age and variability added by measuring methods. Simulations were performed by setting CV1 = CV2 = 0.2 (the "momentary" CV of each subpopulation of parent and daughter cells, respectively). After normalization, the program compared experimental and computed distributions (see reference 2 and Martegaui et al., Cytom-

etry, in press, for a more detailed description). DNA distributions were analyzed by the method of Fried and Mandel (10), which briefly works as follows. (i) The population is separated into compartments, one consisting of G1 cells, another of G2 and M cells, and several of S phase cells which have synthesized different specified fractions of their DNA; (ii) the fluorescence intensity of cells in each compartment is normally distributed with the mean of the G2 + M compartment having a channel location twice that of G1; the S phase compartments have means at intermediate values. The sizes of the compartments, and hence the fraction of cells in each cell cycle phase, are determined by a least-squares fitting procedure involving the observed data, using a computer program implemented on a PDP 11/34 (Digital Equipment Corp.).

Chemical determination of protein content. Samples of ca. 5×10^8 cells were collected by centrifugation and were washed once with cold distilled water and three times with cold 5% trichloroacetic acid. The protein content of the cultures was determined as previously described (23) by the standard microbiuret method. P_s and P_m were calculated by the equations

$$P_s = P_p\, e^{\alpha(T_p - T_\Sigma)} \quad (10)$$

$$P_m = P_p\, e^{\alpha(T_p - T_{G1^*})} \quad (11)$$

P_p, the average protein content of a parent cell at the beginning of a cycle, was calculated as in reference 30:

$$P_p = \frac{\bar{P}}{\alpha(T_P - T_D + T_D\, e^{\alpha T_P})} \quad (12)$$

where $\bar{P}$ is the mean protein content per cell.

RESULTS

Parameters of the nuclear division cycle. DNA distributions were obtained for *S. cerevisiae* populations in balanced exponential growth on different carbon and nitrogen sources in batch cultures at 30°C. The Fried algorithm (10) was used for the deconvolution of the DNA distributions, and the average duration of various cell phases was calculated as indicated above.

The length of the S phase remained constant (approximately 15 min) for duplication times up to 110 min, then it slowly increased as the doubling time of the culture increased (Table 1). The duration of the G2+M phase steadily increased with increasing duplication time. Interestingly, at all growth rates, the budded period was shorter by 5 to 10 min than the sum of S + G2 + M +G1* (T_Σ) phases. This finding indicates that the initiation of DNA replication occurs only a few minutes before the detection of the emergence of the bud. This is not always the case; in a different yeast strain (A364a) in exponential growth or under unbalanced conditions of growth, the two events (budding and onset of DNA replication) are less closely associated; therefore, caution should be taken in using bud emergence as a morphological marker of the entrance into the S phase (23).

TABLE 1. Timing of bud emergence and of initiation of DNA replication

T	T_S[a]	T_{G2+M}[a]	T_{G1^*}[b]	T_Σ[a]	T_B[c]
75	15	35	12	63	58
101	16	54	20	90	84
104	16	47	17	80	80
107	15	58	17	90	85
122	25	59	22	107	98
139	22	69	29	120	113
185	25	96	31	152	139
314	53	74	55	183	170

[a] Cell cycle phases were calculated by using equations 5 to 9 in the text. Percentages of cells in S phase and G2 + M + G1* were determined by deconvolution (10) of the DNA profiles obtained by flow cytometry. Values used are means of an analysis conducted on three independent samples taken at different times during exponential growth. The correct G2 + M fraction was obtained by subtracting the fraction of binucleated cells.

[b] T_{G1^*} was calculated according to equation 7, using values obtained by DAPI staining of nuclei.

[c] T_B was calculated by means of equation 2, using the fraction of budded cells obtained by bud scar analysis.

As duplication time increased, mean cell volume (determined with a Coulter Counter Channelyzer) and average protein content (determined with the standard microbiuret method) decreased in a similar manner (Fig. 1A). Two apparent exceptions were seen in cells growing in YEP-gluconate (T = 185) and YNB-ethanol (T = 314), in which mean protein content and volume, respectively, were abnormally high. The increase in volume in cells growing on ethanol could be due to increased vacuolation, a response often seen in yeast cells in suboptimal growth conditions.

Progression of the nuclear division cycle appears to depend on the reaching of a critical protein level (P_s) for the onset of DNA replication and on the reaching of a critical protein level for the onset of mitosis (P_m,P_m>P_s) and the elapse of a timer (the minimal G2 phase) for nuclear division (1, 3). The determination of the duration of the nuclear phases allows the calculation of P_s and P_m from the average protein content (1, 18). It has been found that the protein level at the initiation of DNA replication is growth modulated, i.e., it is higher at faster growth rates, as reported by other investigators for volume at bud emergence (16, 18, 30). Also, protein content at mitosis (P_m) depends on the growth rate, but the ratio between the two thresholds remains markedly constant at all growth rates (Fig. 1B and C).

Deconvolution of protein distribution functions. Protein distributions of fluorescein isothiocyanate-stained cells taken from exponentially growing populations are easily reproducible. The

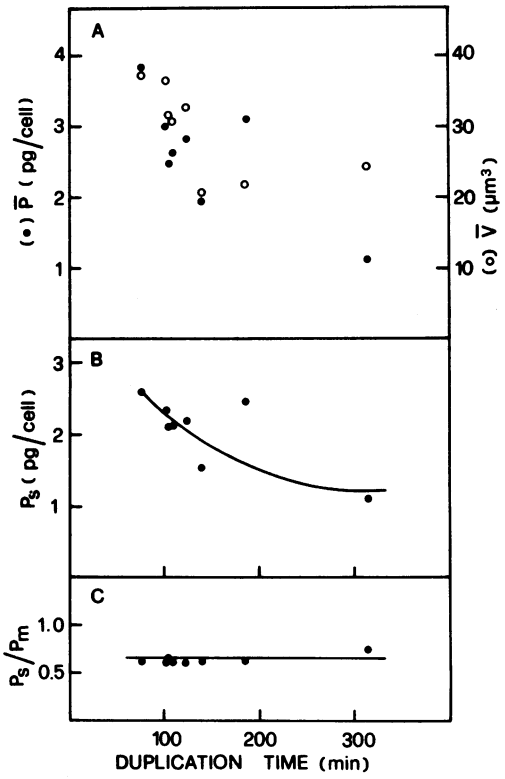

FIG. 1. (A) Mean volume (○) and protein content (●) at different duplication times, measured as described in the text. Both sets of data are means of three independent determinations made on samples taken during exponential growth. Standard deviations were always smaller than 10%. The duplication time of the culture, T (min, = ln2/α), was determined from the rate constant of growth (α) measured as indicated in the text. (B) Protein content required for the initiation of DNA replication, P_s, plotted as a function of duplication time. (C) Ratio between P_s and P_m (the protein content required for mitosis) at different duplication times. P_s and P_m were calculated as described in the text.

shape and CV of the distribution depend on the growth conditions and may have a predictive value on the state of the population, foretelling, for instance, the reaching of an exponential growth condition before it can be assessed by counting the cell number (2). Typical protein distributions are shown in Fig. 2 (closed circles). For duplication times up to 200 min, distributions were unimodal, with a CV of approximately 35 to 40%, whereas at longer duplication times, distributions became bimodal.

Protein distributions were analyzed with a fitting program that accounted for measurement errors and the variability of the momentary size distribution and made the assumption that the protein content, as well as the cell volume at bud emergence, increases at each new generation of parent cells; hence, older parent cells have shorter generation times (16, 19). Computer-generated histograms fit—with fairly good accuracy—protein distributions in balanced exponential growth (Fig. 2), whereas protein distribution functions from the Hartwell and Unger model, which assumes instead that all parent cells have the same generation time regardless of their genealogical age, are not satisfactory (2).

Protein and DNA distributions are a sensitive test to ascertain the establishment of a condition

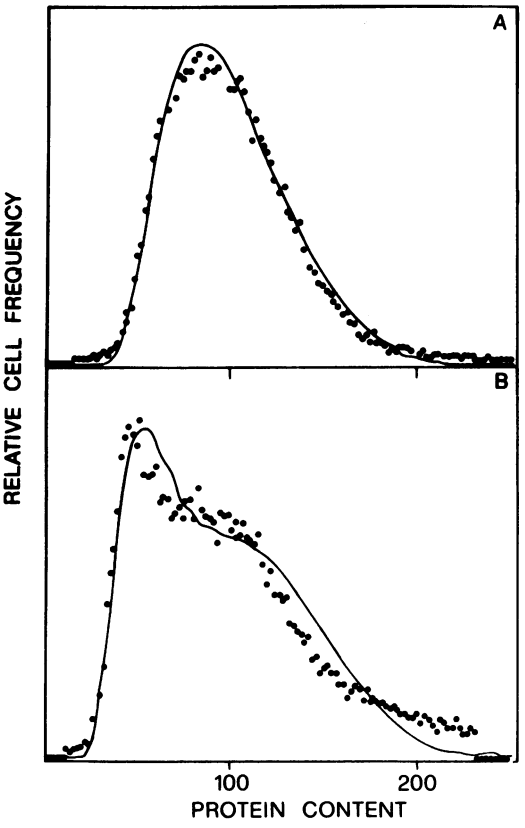

FIG. 2. Fitting of experimental protein distributions of FITC-stained cells obtained for *S. cerevisiae* cells exponentially growing in different media. Circles indicate experimental distributions; lines indicate computed distributions. (A) YEP-maltose; T = 139 min; T_B = 113 min. (B) YNB-ethanol; T = 314 min; T_B = 170 min. Simulations were performed by setting CV1 = CV2 = 0.2, Q = 0.2, and a = 0.5. CV1 and CV2 are the momentary coefficients of variation for each generation of parent and daughter cells, respectively. Q represents the increase of the critical protein level required for bud emergence for parent cells with one bud scar with respect to daughter cells, and $a^{i-1}Q$ represents the increase in this value for parent cells with genealogical age i with respect to parent cells with genealogical age $i - 1$.

of balanced exponential growth, i.e., a growth condition in which "the ages of randomly picked cells are independently distributed according to the stable age distribution of the population" (14). Since the cell age is not easily measured, other cell parameters must be considered. The classical requirement of an exponential increase in cell number is not in itself enough for one to assume that this condition of growth has been established. In fact, *S. cerevisiae* cells grown on YNB with glutamine as a nitrogen source showed an exponential increase in cell number (Fig. 3a) and a constant fraction of unbudded cells, F_U (Fig. 3b, lane 1). Nevertheless, the increase with time in the fraction of G1 cells, F_{G1}, as judged by the Fried analysis of the DNA histograms (Fig. 3b and 4b, lane 2), and the failure of our computer program to fit protein distributions (Fig. 4a), indicate that the population is not in balanced exponential growth.

Thus, protein and DNA distributions strictly related to cell age should be regarded as better indicators of the age structure of yeast cell populations than should cell number or bud emergence.

Structure of the population. Since, as shown above, the protein level at bud emergence appears to increase at each new generation, the cell division cycle of *S. cerevisiae* may be represented as shown in Fig. 5. A population in balanced exponential growth is then composed of subpopulations of parents $P_1, P_2 \ldots .P_i$ and of daughters $D_1, D_2 \ldots .D_i$, where i is the genealogical age which, for parents, is indicated by the number of bud scars. The relative frequencies of the different subpopulations and average parent and daughter generation times may be calculated as indicated in the Appendix. The experimental and the calculated frequencies of parent and daughter cells closely agree with the frequencies estimated by bud scar analysis (Table 2). Also, the calculated average cycle times of parent and daughter cells are almost identical to the cycle times estimated by bud

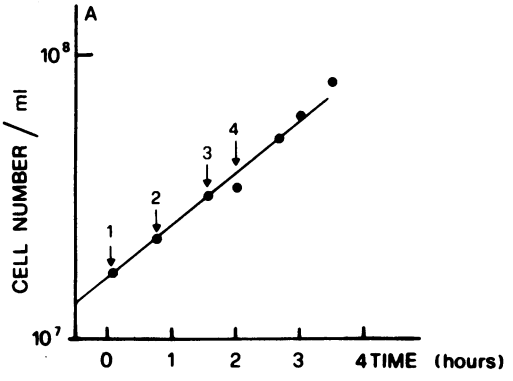

B

	F_U	F_{G_1}
1	0.32	0.26
2	0.34	0.28
3	0.34	0.33
4	0.33	0.37

FIG. 3. (A) Growth curve for *S. cerevisiae* cells on YNB-glutamine. (B) Frequency of unbudded cells (F_U) obtained by direct microscopic examination, and frequency of G1 cells (F_{G1}) derived by the Fried analysis (shown in Fig. 4B) in samples (1 to 4) taken at various times during growth, as indicated by arrows in (A).

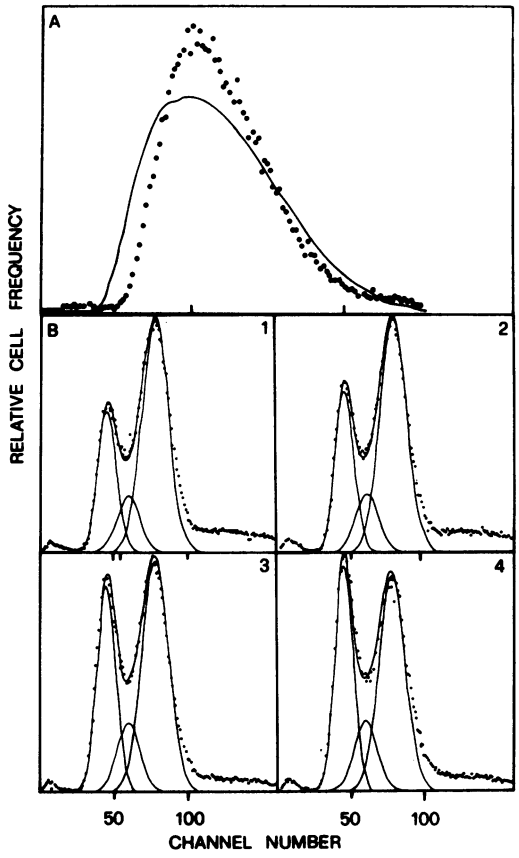

FIG. 4. (A) Attempt to fit protein distribution in unbalanced exponential growth. Cells withdrawn at time 2 during growth of Fig. 3A were stained with FITC and analyzed as usual. Simulations were performed by setting CV1 = CV2 = 0.2. Experimentally determined parameters were T = 97 and T_B = 72. circles indicate experimental distribution; line indicates computed distribution. (B) Analysis, by means of the Fried algorithm, of the DNA distributions obtained by flow cytometry at times indicated by arrows in Fig. 3A.

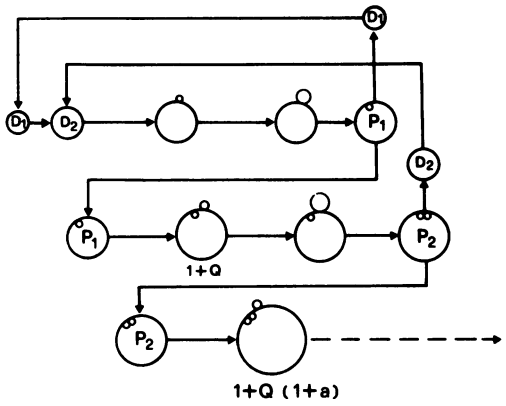

FIG. 5. Model of cell cycle of different genealogically aged parents (P_i) and daughters (D_i). All daughter cells begin to bud at a relative protein content of 1, independently of the genealogical age of their parents. On the contrary, the critical protein level required for parent cells to bud increased by an a^{i-1} Q factor of each generation and thus had a value of 1 + Q for first-generation parents, 1 + Q (1 + a) for second-generation, etc. Since the budded period is of constant duration at each genealogical age, genealogically older parent cells and their daughters are larger at division. Hence, P_2 and D_2 cells are shown here to begin their cycle on the right of P_1 and D_1, respectively, to indicate their larger protein content.

scar analysis (Table 2). To have a better understanding of the degree of heterogeneity derived from the increase in the threshold protein level for bud emergence with genealogical age, the results shown in Table 3, which shows the cycle time and the frequency of daughters (D_1 to D_4) and parents (P_1 to P_4), may be useful. There is a rather sharp decrease in cycle times of older parent and daughter cells with respect to first-generation parents and daughters. At all tested growth rates, the percentage of first-generation parents was almost identical to the sum of subsequent generation parents, and the budded period was shorter than the parent cycle time, particularly for the younger and more frequent genealogical ages. This means that after cell division, parent cells are not immediately ready to undertake a new cycle and have to traverse a G1 period, which decreases in length at increasing genealogical age. The increase in cell mass of the parent cells with genealogical age causes an increase in the cell size at birth of the daughters. Accordingly, the cycle times of the daughters decrease with genealogical age (Table 3).

DISCUSSION

The integration of the well-known bud scar analysis with the mathematical analysis of the DNA and protein distributions, obtained by flow microfluorometry, is the element of novelty of this paper. It allows a deeper understanding of the relations between growth metabolism and the nuclear division cycle in budding yeasts. Flow cytometric techniques are a powerful tool for cell cycle analysis: in fact, small differences in the kinetics of growth of individual cells and slight variations in the structure of the population are easily detected, in a statistically significant manner, by flow microfluorometry in unperturbed populations in balanced exponential growth. Size density functions introduce a process of amplification for the detection of differences in the kinetics of single cell growth: in fact, small differences between linear and exponential growth kinetics over a cell cycle result in a much more pronounced difference between the respective size density functions (33). The analysis of protein distributions of exponentially growing cells may thus be more informative in the assessment of cell growth kinetics than the direct observation of single cells or of perturbed "synchronous" cultures (16, 21, 22). Instead, for instance, the determination of the average cycle times of parent and of daughter cells does

TABLE 2. Experimental and theoretical frequency and cycle time of parent and daughter cells[a]

T	F_P		T_P		T_D		F_D	
	By bud scar analysis	Calculated	By bud scar analysis	Calculated	By bud scar analysis	Calculated	By bud scar analysis	Calculated
75	0.41	0.48	69	71	81	84	0.59	0.52
101	0.42	0.49	96	103	108	110	0.58	0.51
104	0.41	0.48	94	99	112	117	0.59	0.52
107	0.42	0.49	99	104	114	117	0.58	0.51
122	0.44	0.47	113	115	132	135	0.56	0.53
139	0.54	0.49	130	137	148	151	0.55	0.51
185	0.44	0.47	173	178	197	198	0.56	0.53
314	0.46	0.38	220	224	432	476	0.54	0.62

[a] Values of parent and daughter frequency and average cycle times were computed by using experimental α and T_B and values of Q = 0.2 for all duplication times tested, except for T = 122, for which we used Q = 0.15 and a = 0.5, which gave the best fit to protein distributions.

TABLE 3. Structure of yeast populations growing at different growth rates

T	T_B	Parent and daughter cell generation times[a]								Parent and daughter cell frequencies[b]							
		T_{P_1}	T_{P_2}	T_{P_3}	T_{P_4}	T_{D_1}	T_{D_2}	T_{D_3}	T_{D_4}	F_{P_1}	F_{P_2}	F_{P_3}	F_{P_4}	F_{D_1}	F_{D_2}	F_{D_3}	F_{D_4}
75	58	77	66	62	60	95	75	66	62	0.27	0.12	0.06	0.03	0.30	0.13	0.06	0.03
101	84	110	95	89	86	123	96	84	84	0.28	0.12	0.06	0.03	0.30	0.12	0.06	0.03
104	80	107	92	86	83	131	104	92	87	0.27	0.12	0.06	0.03	0.30	0.13	0.06	0.03
107	85	113	97	91	88	132	104	92	86	0.28	0.12	0.06	0.03	0.30	0.12	0.06	0.03
122	98	123	109	104	101	149	124	113	108	0.26	0.12	0.06	0.03	0.30	0.13	0.07	0.04
139	113	149	129	120	116	168	132	116	113	0.28	0.12	0.06	0.03	0.30	0.12	0.06	0.03
185	139	187	160	149	144	235	187	166	156	0.26	0.12	0.06	0.03	0.30	0.13	0.06	0.04
314	170	253	206	187	178	530	449	410	393	0.19	0.09	0.06	0.04	0.30	0.16	0.10	0.06

[a] Generation times of different genealogically aged parent and daughter cells were calculated by using equations A4 and A5.

[b] Frequencies of different genealogically aged parent and daughter cells were calculated by using equations A12 and A13.

not enable one to discriminate between two different age structures, i.e., that derived from the Hartwell and Unger model and that derived from our model, which implies a much larger heterogeneity in both parent and daughter cell populations (Tables 2 and 3). Since the size distribution derived from the classical unequal division model fails to fit protein distributions, because the theoretical distribution is not dispersed enough (2), the increase in volume at budding for genealogically older cells (16) appears to be accompanied by an increase in protein content.

The cell division cycle in budding yeast cells appears, therefore, to take place as shown in Fig. 5 and 6. This mechanism of cell division generates a large variability in populations of *S. cerevisiae* cells in balanced exponential growth, which then become composed of subpopulations of parents and daughters that have progressively shorter cycle times and that are less frequent at increasing genealogical age (Table 3). This structure of the population accounts for several observations made in budding yeast cell populations that do not find a completely satisfactory interpretation in the classical unequal division model, which yields only two subpopulations, parents and daughters (13, 20), which are briefly described here.

Steady states of growth are generated in which the parent cell contributes the mass accumulated during the budded period to its daughter at division and, in the meantime, parent cells increase in size in successive generations, as previously observed (13).

Parent cells grow before the next bud initiation at all growth rates. Parents are predicted to spend a longer time as unbudded at slow growth rates than at fast growth rates (Table 3), although in a less marked way than daughters, as observed previously (18, 29).

In our experiments, the budded period considerably expanded at longer duplication times, as reported by other authors for cells whose growth rate was changed by limiting nutrient concentration in a chemostat (29). This behavior has been tentatively ascribed to catabolite derepression, although there is no biochemical indication of how a change in metabolism may affect cell cycle progression. However, it could be more satisfactorily interpreted in the frame of the cell size model developed in our laboratory: it holds that cell cycle progression requires the attainment of two threshold protein levels, one controlling the entrance in the S phase and the other controlling mitosis. In fact, in all growth conditions, the protein level at the beginning of mitosis is increased by the same percentage as that of the protein level at the onset of DNA replication, which suggests that both thresholds are nutritionally modulated, but in such a way that their ratio remains constant at all growth rates. The larger part of the budded period increase is observed in the post-replicative phase, although at longer duplication times, the S phase also expands. A more dramatic increase in the S phase has been reported by other authors using a different strain (A364a) and an autoradiographic technique (26), whereas a study using flow microfluorometry to investigate the yeast cell cycle found that the S phase duration remains con-

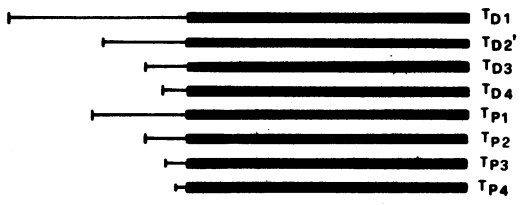

FIG. 6. Graphic representation of the cycle times of different genealogically aged parents and daughters (T_{P_i} and T_{D_i}). Heavier lines represent the budded phase, common to both parent and daughter cells and independent of genealogical age; thinner lines indicate the unbudded period, progressively shorter in genealogically older cells.

stant at all but the lowest growth rates (17, 28). In fact, such differences could be due to the different methods used to analyze DNA histograms, which, especially with large CVs (about 10%), may yield different results, and to the different strain and temperature used.

The budded period is found to be shorter by 5 to 10 min than T_Σ, i.e., DNA replication initiates when cells are still unbudded, or at least appear as unbudded under a light or fluorescence microscope. Such a difference could depend on the different sensitivities of the methods of detection, but it also depends on strain, temperature, and methods employed to alter the growth rate. By the use of low doses of cycloheximide on strain A364a at 24°C, much more pronounced differences have been measured (23).

The percentage of first-generation parents predicted by our model is very close, or even identical, to the sum of subsequent-generation parents (Table 3); therefore, this finding cannot be taken as an indication that the generation time of parents is independent of genealogical age, as previously proposed (5). A trend for larger parent cells to produce larger daughter cells has been observed (13), and it is explained by our model.

The cycle times of both parents and daughters as a function of the genealogical age have not been extensively investigated. Uncertainty in comparing results on this aspect of the cell cycle of budding yeast cells is compounded by the fact that in time-lapse experiments, cells that are budding for their first time—as well as cells (in decreasing proportion) that are budding for their second and third time, etc. (13)—are all called first-generation parents. A recent careful study indicated that second-generation daughters have shorter cycle times than first-generation daughters (32; Table 3).

The model discussed in this paper holds that there is a cell size control on budding: it has often been suggested that a cell may do so by monitoring a specific protein whose synthesis is correlated with overall growth and that triggers cell cycle progression when it reaches a critical level (9). The assumption that such an activator protein first titrates an inhibitor, whose presence is suggested by several experimental findings (25, 31), and then activates the cell cycle progression, has been developed in a model (L. Alberghina, E. Martegani, L. Mariani, and G. Bortolan, submitted for publication). Interestingly, this mathematical model predicts for unequally dividing cells an increase in protein content at bud initiation for cells of increasing genealogical age, in agreement with the findings reported in this paper, and thereby suggests a possible molecular mechanism for the increase in the protein threshold with genealogical age.

ACKNOWLEDGMENTS

We thank G. Frascotti for skillful technical assistance, and E. Martegani and L. Mariani for helpful discussions and suggestions.

This work was partially supported by grant no. CT 82.02008 from the Consiglio Nazionale delle Ricerche, Rome.

APPENDIX

The model for unequally dividing yeast cell populations used in this paper differs from that originally proposed by Hartwell and Unger (13) in that it makes the further assumption that protein level at bud emergence increases at each new generation, as suggested by the observed increase in cell volume at the onset of budding (16). Basic assumptions and relations may be summarized as follows.

(i) Protein growth dynamics are described by exponential functions (8, 27).

(ii) A critical protein level P_{ci}, whose value increases with the genealogical age i, is required for bud emergence and for the beginning of DNA replication. More precisely, taken as 1, the critical protein level for daughter cells, i.e., $P_{c0} = 1$, the protein content at bud emergence for ith-generation parent cells is given by:

$$P_{ci} = 1 + Q(1 + a + \ldots\ldots + a^{i-1}) \qquad \text{(A1)}$$

with $Q < 1$ and $a < 1$, where Q represents the increase in value of the critical protein content for parent cells with one bud scar with respect to daughter cells, and $a^{i-1}\,Q$ represents the increase in such level for cells with genealogical age (i) with respect to cells with genealogical age ($i-1$).

(iii) At any given growth rate, the budded period (T_B) is appreciably constant for both mother and daughter cells.

(iv) At division, the protein synthesized during the budded phase is given to the bud.

With these assumptions, the normalized protein contents for parent cells P_i and their daughter cells D_i are given by:

$$p_{pi}(\tau) = 1 + Q(1 + a + \ldots + a^{i-1})\, e^{\alpha(T_B - \tau)} \qquad 0 \le \tau \le T_{pi} \qquad \text{(A2)}$$

$$p_{Di}(\tau) = e^{\alpha(T_B - \tau)} \qquad 0 \le \tau \le T_{Di} \qquad \text{(A3)}$$

with the generation times for ith generation of parent and daughter T_{Pi} and T_{Di} given by:

$$T_{Pi} = T_B + \frac{1}{\alpha} \ln \frac{(1 - a) + Q(1 - a^i)}{(1 - a) + Q(1 - a^{i-1})} \qquad \text{(A4)}$$

$$T_{Di} = T_B - \frac{1}{\alpha} \ln \left[\left(1 + Q \frac{1 - a^{i-1}}{1 - a} \right) (e^{\alpha T_B} - 1) \right] \qquad \text{(A5)}$$

more exactly, so that also for very great values of i, $T_{Di} \ge T_B$, the following assumption (v) must be made:

$$\frac{Q}{1 - a} \le \frac{2 - e^{\alpha T_B}}{e^{\alpha T_B} - 1}$$

(vi) If the cell population is in balanced steady state of exponential growth, then

(vii) there is no cell loss in the population, and (viii) the critical protein level p and therefore the duration of the generation times depend only on genealogical age; the ideal age and protein density functions may thus be derived. The age density function $n_{Pi}(\tau)$; $n_{Di}(\tau)$ of the different subpopulations can be expressed as a function of a normalization factor (A), whose value can be computed to satisfy:

$$\sum \left[\int_0^{T_{Pi}} n_{Pi}(\tau)\, d\tau + \int_0^{T_{Di}} n_{Di}(\tau)\, d\tau \right] = 1 \quad \text{(A6)}$$

and is given by:

$$n_{Pi}(\tau) = \frac{Ae^{-(i-1)\alpha T_B} e^{\alpha\tau}}{[1 + Q(1 + a + \ldots a^{i-1})](e^{\alpha T_B} - 1)}$$

$$0 \le \tau \le T_{Pi} \quad \text{(A7)}$$

$$n_{Di}(\tau) = Ae^{-(i-1)\alpha T_B} \quad e^{\alpha\tau}\ 0 \le \tau \le T_{Di} \quad \text{(A8)}$$

with $i = 1,2,3 \ldots\ldots$ and T_{Pi} and T_{Di} as given by equations A4 and A5. Starting from equations A2, A3, A7, and A8, the protein density functions of the various subpopulations can be derived as

$$n(p) = n\,[\tau(p)] \cdot (-d\tau/dp) \quad \text{(A9)}$$

and are given by

$$n_{Pi}(p) = \frac{Ae^{-(i-2)\alpha T_B}}{\alpha(e^{\alpha T_B} - 1)} \cdot \frac{1}{p^2} \quad \text{(A10)}$$

$$[1 + Q(1 + a + \ldots + a^{i-2})]$$

$$\le p \le [1 + Q(1 + a + \ldots\ a^{i-1})]\, e^{\alpha T_B}$$

$$n_{Di}(p) = \frac{Ae^{-(i-2)\alpha T_B}}{\alpha P^2} \quad \text{(A11)}$$

$$[1 + Q(1 + a + \ldots + a^{i-2})\, e^{\alpha T_B} - 1)] \le P \le e^{\alpha T_B}$$

The frequency of each generation of parent and daughter cells is given by:

$$F_{Pi} = \int_0^{T_{Pi}} n_{Pi}(\tau)\, d\tau \Big/ \sum \int_0^{T_{Pi}} n_{Pi}(\tau)\, d\tau \quad \text{(A12)}$$

$$F_{Di} = \int_0^{T_{Pi}} n_{Di}(\tau)\, d\tau \Big/ \sum \int_0^{T_{Pi}} n_{Di}(\tau)\, d\tau \quad \text{(A13)}$$

Average parent and daughter generation times are thus given by

$$T_P = \sum T_{Pi} \cdot F_{Pi} \quad \text{(A14)}$$

$$T_D = \sum T_{Di} \cdot F_{Di} \quad \text{(A15)}$$

The preceding equations have been used in this paper to analyze protein distributions and to determine the structure of yeast cell populations in balanced exponential growth.

LITERATURE CITED

1. **Alberghina, L., L. Mariani, and E. Martegani.** 1980. Analysis of a model of cell cycle in eucaryotes. J. Theor. Biol. **87**:171–188.
2. **Alberghina, L., L. Mariani, E. Martegani, and M. Vanoni.** 1983. Analysis of protein distribution in budding yeast. Biotechnol. Bioeng. **25**:1295–1310.
3. **Alberghina, L., and E. Sturani.** 1981. Control of growth and of the nuclear division cycle in *Neurospora crassa*. Microbiol. Rev. **45**:99–122.
4. **Bailey, J. E., J. Fazel-madiljessi, D. N. McQuitty, and M. F. Gilbert.** 1979. Measuring microbial population dynamics. Ann. N.Y. Acad. Sci. **326**:7–16.
5. **Carter, B. L. A.** 1981. The control of cell division in *Saccharomyces cerevisiae*, p. 99–117. In P. C. L. John (ed.), The cell cycle. Cambridge University Press, Cambridge, England.
6. **Carter, B. L. A., and M. N. Jagadish.** 1978. Control of cell division in the yeast *Saccharomyces cerevisiae* cultured at different growth rates. Exp. Cell. Res. **112**:373–383.
7. **Crissman, H. A., and J. A. Steinkamp.** 1973. Rapid simultaneous measurement of DNA, protein and cell volume in single cells from large mammalian cell populations. J. Cell. Biol. **59**:766–771.
8. **Elliott, S. G., and C. S. McLaughlin.** 1978. Rate of macromolecular synthesis through the cell cycle of the yeast *Saccharomyces cerevisiae*. Proc. Natl. Acad. Sci. U.S.A. **75**:4384–4388.
9. **Fantes, P. A., W. D. Grant, R. H. Pritchard, P. E. Sudberry, and A. E. Wheals.** 1975. The regulation of cell size and the control of mitosis. J. Theor. Biol. **50**:213–244.
10. **Fried, J., and M. Mandel.** 1979. Multi-user system for analysis of data from flow-cytometry. Comput. Programs Biomed. **10**:218–230.
11. **Gray, J. W., and P. N. Dean.** 1980. Display and analysis of flow-cytometric data. Annu. Rev. Biophys. Bioeng. **9**:509–539.
12. **Hartwell, L. H.** 1974. *Saccharomyces cerevisiae* cell cycle. Bacteriol. Rev. **38**:164–198.
13. **Hartwell, L. H., and M. Unger.** 1977. Unequal division in *Saccharomyces cerevisiae* and its implications for the control of cell division. J. Cell Biol. **75**:422–435.
14. **Jagers, P.** 1978. Balanced exponential growth: what does it mean and when is it there?, p. 21–29. *In* A. J. Valleron and P. D. M. McDonald (ed.), Biomathematics and cell kinetics. Elsevier/North-Holland Biomedical Press, Amsterdam.
15. **James, T. W., P. Hemond, G. Czer, and R. Bohman.** 1975. Parametric analysis of volume distributions of *Schizosaccharomyces pombe* and other cells. Exp. Cell Res. **94**:267–277.
16. **Johnston, G. C., C. W. Ehrhardt, A. Lorincz, and B. L. A. Carter.** 1979. Regulation of cell size in the yeast *Saccharomyces cerevisiae*. J. Bacteriol. **137**:1–8.
17. **Johnston, G. C., R. A. Singer, S. O. Sharrow, and M. L. Slater.** 1980. Cell division in the yeast *Saccharomyces cerevisiae* growing at different rates. J. Gen. Microbiol. **118**:479–484.
18. **Lord, P. G., and A. E. Wheals.** 1980. Asymmetrical division of *Saccharomyces cerevisiae*. J. Bacteriol. **142**:808–818.
19. **Lord, P. G., and A. E. Wheals.** 1981. Variability in individual cell cycles of *Saccharomyces cerevisiae*. J. Cell. Sci. **50**:361–376.
20. **Lord, P. G., and A. E. Wheals.** 1983. Rate of cell cycle initiation of yeast cells when cell size is not a rate-determining factor. J. Cell Sci. **59**:183–201.
21. **Mitchison, J. M.** 1971. The biology of cell cycle. Cambridge University Press, Cambridge, England.

22. **Mitchison, J. M.** 1981. Changing perspectives in the cell cycle, p. 1–10. *In* P. C. L. John (ed.), The cell cycle. Cambridge University Press, Cambridge, England.
23. **Popolo, L., M. Vanoni, and L. Alberghina.** 1982. Control of the yeast cell cycle by protein synthesis. Exp. Cell Res. **142**:69–78.
24. **Pringle, J. R., and L. H. Hartwell.** 1981. The *Saccharomyces cerevisiae* cell cycle. Cold Spring Harbor Monogr. Ser., p. 97–142.
25. **Pritchard, R. H.** 1978. Control of DNA replication in bacteria, p. 1–27. *In* I. Molineux and M. Kohivama (ed.), the DNA synthesis, present and future. Plenum Press, New York.
26. **Rivin, C. J., and W. L. Fangman.** 1980. Cell cycle phase expansion in nitrogen-limited cultures of *Saccharomyces cerevisiae*. J. Cell Biol. **85**:96–107.
27. **Ronning, O. W., E. O. Pettersen, and P. O. Seglen.** 1979. Protein synthesis and protein degradation through the cell cycle of human NHIK 3025 cells in vitro. Exp. Cell Res. **123**:63–72.
28. **Slater, M. L., S. O. Sharrow, and J. J. Gart.** 1977. Cell cycle of *Saccharomyces cerevisiae* in populations growing at different rates. Proc. Natl. Acad. Sci. U.S.A. **74**:3850–3854.
29. **Thompson, P. W., and A. E. Wheals.** 1980. Asymmetrical division of *Saccharomyces cerevisiae* in glucose-limited chemostat culture. J. Gen. Microbiol. **121**:401–409.
30. **Tyson, C. B., P. G. Lord, and A. E. Wheals.** 1979. Dependency of size of *Saccharomyces cerevisiae* cells on growth rate. J. Bacteriol. **138**:92–98.
31. **Tyson, J., G. Garcia-Herdurgo, and W. Sachsenmaier.** 1979. Control of nuclear division in *Phisarum polycephalum*. Exp. Cell Res. **119**:87–98.
32. **Wheals, A. E.** 1982. Size control models of *Saccharomyces cerevisiae* cell population. Mol. Cell. Biol. **2**:361–368.
33. **Williams, F. M.** 1971. Dynamics of microbial populations, p. 198–268. In B. C. Patten (ed.), System analysis and simulation in ecology, vol. 1. Academic Press, Inc. N.Y.